Designing chitosan-tripolyphosphate microparticles with desired size for specific pharmaceutical or forensic applications

Ezzeddin M. A. Hejjaji[a,b], Alan M. Smith[b] and Gordon A. Morris[a, ✉]

[a]Department of Chemical Sciences, School of Applied Sciences, University of Huddersfield, Huddersfield HD1 3DH, UK

[b]Department of Pharmacy, School of Applied Sciences, University of Huddersfield, Huddersfield HD1 3DH, UK

✉Corresponding author

Tel: +44 (0) 1484 473871

Fax: +44 (0) 1484 472182

Email: g.morris@hud.ac.uk

Highlights

- CS: TPP microparticles were prepared using an experimental design
- Variable factors were pH, ionic strength and CS: TPP ratio
- Physical properties ([η], ζ-potential and $D_{[4,3]}$) were measured
- Equations were generated to predict physical properties of the microparticles
- Potential to design tuneable CS-TPP microparticles for specific applications

Abstract

Chitosan (CS) is a natural cationic polymer obtained by the partial *N*-deacetylation of chitin. Chitosan microparticles can be prepared by cross-linking with tripolyphosphate (TPP) via the ionic interaction between positively charged amino groups (CS) and negatively charged counter ions (TPP). This can be controlled by the charge density of CS and TPP, which depend on the pH and ionic strength of the solution. The purpose of this study is to investigate the combined effects of three independent variables (pH, ionic strength and CS: TPP ratio) on three important physico-chemical properties (viscosity, zeta potential and particle size) during the preparation of microparticles. CS: TPP microparticles were prepared using experimental design and equations were generated and used to predict relative viscosity, zeta potential and particle size under different conditions. This gives us the ability to design tuneable CS-TPP microparticles with desired size for specific pharmaceutical or forensic applications *e.g.* latent fingerprint visualisation.

Keywords: Chitosan-Tripolyphosphate Microparticles; Ionic gelation; Experimental design

1. Introduction

Chitosan refers to a family of linear copolymer polysaccharides consisting of β (1-4)-linked 2-amino-2-deoxy-D-glucopyranose (D-glucosamine) and 2-acetamido-2-deoxy-D-glucose (*N*-acetyl-D-glucosamine) units with different fractions of acetylated units [1]. An acetyl group may be present on some units (*N*-acetyl- D-glucosamine), which determines the degree of deacetylation (DD). Moreover, the DD of commercial chitosan is approximately 66 - 95 %, and the molecular weight (M_W) approximately 10000 – 1000000 g/mol [2]. The structural units of chitosan have one reactive primary amino group (-NH_2) on the C-2 position of each D-glucosamine unit, and two reactive free hydroxyl groups (-OH) for each C-6 and C-3 position building unit (glucosamine and *N*-acetyl-D-glucosamine). These groups (both amino and hydroxyl) can be modified to obtain different chitosan derivatives, and provide opportunities for chemical modification to impart useful physicochemical properties and distinctive biological functions [3]. In addition, the advantage of chitosan over other polysaccharides is that its chemical structure allows specific modifications at the C-2 position without too many difficulties [4]. Chitosan has been investigated widely for its potential in the development of drug delivery systems and pharmaceutical applications [5] and more recently for its forensic applications [6].

In latent fingerprint visualisation it is now accepted that particles adhere to fingermarks due to the mechanical attraction with the oily subcutaneous residues [7]. The factors with influence this interaction are particle size, particle charge, particle shape and relative surface area [7, 8] all of which are controlled by processing parameters such as chitosan concentration, pH and ionic strength of the dissolution media, temperature of cross-linking, stirring rate, *etc* [9].

Various techniques have been developed to prepare chitosan micro/nanoparticles, such as ionic gelation, emulsion droplet, spray drying, coacervation and self-assembly chemical modification [10]. Among those methods, the ionic gelation method (also known as ionotropic gelation) with the non-toxic multivalent polyanion tripolyphosphate (TPP) is the most widely used approach to physical cross-linking. Ionic cross-linking can occur inside the network via interactions between the negative charges of the cross-linker such as TPP and the positively charged amino groups of chitosan molecules [11-14]. This method is advantageous as the reaction is simple and the conditions are relatively mild and do not require the use of organic solvents or high temperatures [1, 15]. Other advantages from the point of view of drug delivery and latent fingerprint enhancement are that particle size and (positive) charge can be easily

controlled and microparticle formulations have previously demonstrated the ability to associate with peptides, proteins [16] and with subcutaneous secretions in fingerprints [6].

Knowledge of viscosity, zeta potential, particle size and shape has an influence on potential applications of chitosan-TPP microparticles in drug delivery [9] or in forensic applications [6]. It is therefore the purpose of the present study is to investigate the systematic manipulation of three independent processing parameters (pH, ionic strength and CS: TPP ratio) on three important physico-chemical properties (relative viscosity, zeta potential and particle size) during the preparation of chitosan-TPP (CS-TPP) microparticles. This will then enable the use of mathematical models obtained to predict the relative viscosity, zeta potential (net surface charge) and particle size under different conditions to obtain predicable and programmable microparticle properties in relation to, for example, latent fingerprint enhancement, drug release kinetics or mucoadhesion.

2. Materials and Methods

2.1. Materials

Chitosan of medium molecular weight (M_η ~295 000 g/mol) was obtained from Sigma–Aldrich (Gillingham, UK) and reported to have an average degree of deacetylation (DD) of ~75–85%. Glacial acetic acid, sodium acetate trihydrate and tripolyphosphate (TPP) sodium salt were obtained from Sigma–Aldrich (Gillingham, UK) and red food colouring was from Silver Spoon (Peterborough, UK). All materials were used without any further purification.

2.2. Sample preparation

Nine different acetate buffers (AB) including AB-1, AB-2, AB-3, AB-4, AB-5, AB-6, AB-7, AB-8, and AB-9 were prepared (**Table 1**) in order to investigate the effect of three independent variables: pH value, ionic strength and volumetric ratio of chitosan to TPP on the physico-chemical properties of CS-TPP microparticles.

Table 1. Acetate buffers of varying ionic strength and pH. Buffers AB-1 to AB-9 were used to create generate model equations and buffer AB-10 to AB-13 were used in model validation.

Acetate buffer (AB)	pH	Ionic strength (IS)
AB-1	3.3	0.1 M
AB-2	3.3	0.3 M
AB-3	3.3	0.5 M
AB-4	4.3	0.1 M
AB-5	4.3	0.3 M
AB-6	4.3	0.5 M
AB-7	5.3	0.1 M
AB-8	5.3	0.3 M
AB-9	5.3	0.5 M
AB-10	3.8	0.2 M
AB-11	3.8	0.4 M
AB-12	4.8	0.2 M
AB-13	4.8	0.4 M

2.2.1. Preparation of chitosan and TPP samples with different ionic strengths and pH value (Acetate buffers AB-1 to AB-9)

Nine different chitosan solutions were prepared by dissolving 2 g of chitosan powder in 1 L of acetate buffers (AB-1 to AB-9) to prepare chitosan solutions (2.0 mg/mL). The chitosan solutions were stirred overnight at room temperature using a magnetic stirrer. The TPP powder (1.680 g) was dissolved in 2 L of the acetate buffers (AB) to prepare nine samples of TPP solution (0.84 mg/mL) [17, 18].

2.2.2. Preparation of CS: TPP microparticles

To prepare the CS:TPP microparticles, an appropriate volume of the TPP solution was added drop wise to the appropriate volume of the chitosan solution make seven ratios of CS: TPP microparticles (6:1, 4:1, 2:1, 1:1, 1:2, 1:2, 1:4 and 1:6), and the samples were then stirred at 600 rpm for 60 minutes at room temperature. The resultant microparticles spontaneously formed due to the ionic crosslinking of chitosan by sodium tripolyphosphate. Then 30 drops (~ 2 mL) of red dye added to all ratios to make the particles clearly visible and more amenable in latent fingerprint visualisation. The resultant microparticles were left standing overnight at room temperature before being subjected to further analysis.

2.2.3. Model validation (prediction method)

Chitosan solutions were prepared by dissolving 2 mg/mL of polymer in a further four different acetate buffers (AB-10, AB-11, AB-12 and AB-13) (**Table 1**) and TPP solutions were prepared by dissolving TPP at a concentration of 0.84 mg/mL in the same acetate buffers (AB-10, AB-11, AB-12 and AB-13). The resultant solutions were as in section 2.2.2 to give CS: TPP volume ratios (v/v) of 6: 1, 4: 1, 2: 1, 1: 1, 1: 2, 1: 4 and 1: 6 respectively.

2.3. Characterisation of chitosan microparticles

2.3.1. Fourier transform infrared (FTIR) spectroscopy

FTIR spectra of chitosan, TPP and chitosan microparticles were recorded using a Fourier transform infrared spectrophotometer (Thermo Nicolet 380 FT-IR spectrometer, Thermo Electron Corporation), operating from 4000 to 500 cm^{-1}.

2.3.2. Powder X-Ray diffraction (XRD) study

A crystallinity study was carried out by comparing XRD spectrum of microparticles using Bruker AXS diffractometer (D2 PHASER) with Cu Kα radiation to characterise chitosan, TPP and CS/TPP microparticles. The data was recorded at 2θ range of 5° to 100° at a scanning rate of 4°/min.

2.3.3. Determination of relative viscosities

All rheological measurements (solutions and reference solvents) were performed using a Bohlin Gemini HR Nano Rheometer (Malvern Instruments, Worcester-shire, UK) using 1 mm gap and 55 mm parallel plate geometry at a constant shear rate of 500 s^{-1} under precise temperature control (25.0 ± 0.1°C). All measurements were performed in triplicate.

$$\eta_{rel} = \left(\frac{\eta}{\eta_0} \right) \quad (1)$$

where η is the average (n = 3) viscosity of the CS: TPP microparticles and, η_o is the viscosity for the appropriate acetate buffer [19].

2.3.4. Determination of zeta potential

Zeta potential was measured for each volume ratio using a Malvern Zetasizer NANO-Z (Malvern Instruments Limited, Malvern, UK). All Measurements were performed in the appropriate buffers in triplicate by using a folded capillary cell at 25.0 ± 0.1 ^{o}C and refractive index of the CS: TPP microparticles was set at 1.6 - 1.8 [20] and no significant effect of refractive index was identified. Each data value is an average of three measurements with a refractive index of 1.8.

2.3.5 Determination of particle size

The particle size distributions of the resultant chitosan particles were measured directly by a dynamic light scattering using a Malvern Mastersizer 2000 (Malvern Instruments Ltd., Malvern, UK).The microparticles were dispersed in deionized water. Refractive index of particles and dispersion medium (water) was set to 1.8 (see section 2.3.4) and 1.330, respectively. The size was described using the volume-weighted mean diameter $D_{[4,3]}$. The intensity of scattered light was transformed into the diffusion factor, the mean value of 10 measurements was obtained and each formulation and was repeated three times.

2.3.6. Scanning electron microscopy (SEM)

The surface microparticle morphology was characterised using scanning electron microscopy (SEM). The microparticles were vacuum dried, coated with gold palladium and observed microscopically (JEOL JSM 6060 LV - Oxford instruments, Abingdon, UK). Images were taken by applying an electron beam accelerating voltage of 20 kV. Images were then analysed using Image J software (version 1.42q, National Institute of Health, Bethesda, USA) to estimate particle surface areas.

3. Results and Discussion

3.1. FTIR analysis

The FTIR spectrum of pure TPP (**Figure 1a**) showed characteristic bands at 1217 cm^{-1} which indicates P= O stretching [21], 1138 cm^{-1} which indicates symmetrical and asymmetric stretching vibration of the PO_2 groups , 1094 cm^{-1} which indicates symmetric and asymmetric stretching vibration of the PO_3 groups and 892 cm^{-1} (P- O- P) asymmetric stretching [22]. As ca be seen in **Figure 1b** the spectrum of CS exhibits characteristic absorption bands at 3424 cm^{-1} indicates the combined broad non-symmetric band of the -NH and -OH group stretching vibration of functional groups involved in hydrogen bonds, and the peak at 2873 cm^{-1} indicates

the –CH stretching vibration [21, 23]. The peak at 1650 cm^{-1} indicates C=O stretching in amide I vibration group ($CONH_2$), and 1560 cm^{-1} which indicates N-H deformation in amide II group vibration (NH_2) [24]. Peaks at 1377 cm^{-1} and 1322 cm^{-1} might be attributed to O–H deformation of $–CH_2–OH$ and –CH–OH, and absorption bands at 1151 cm^{-1} indicates asymmetric bridge oxygen (C–O–C) stretching [24].

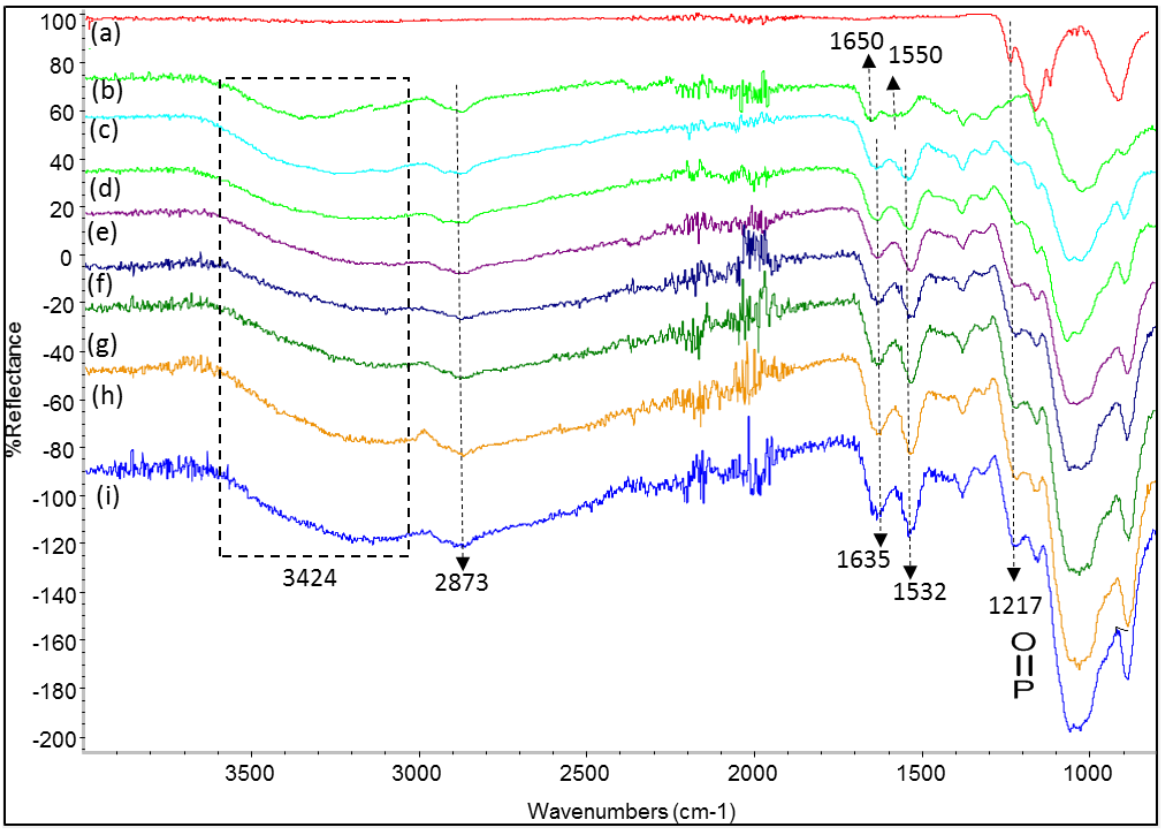

Figure 1. FTIR spectrum of (a) TPP, (b) CS, (c) CS: TPP (6:1), (d) CS: TPP (4:1), (e) CS: TPP (2:1), (f) CS: TPP (1:1), (g) CS: TPP (1:2), (h) CS: TPP (1:4), (i) CS: TPP (1:6) in buffer AB-1.

The CS: TPP particles were characterized through FTIR spectroscopy, and the spectra are presented in **Figures 1c – 1i**. Crosslinking process in the spectra of all CS:TPP ratios samples the band of 3424 cm^{-1} becomes wider, this indicates that hydrogen bonding is enhanced [25]. In addition in microparticles the band of 1650 cm^{-1} disappears and there appears a new band at 1635 cm^{-1}. This band can be assigned to anti-symmetric deformation $N^{-}H$ vibrations in NH^{3+} ion. The 1560 cm^{-1} peak in pure chitosan shifts to a new sharp peak at 1532 cm^{-1} [25]. These two new peaks as mentioned above (1635 cm^{-1} and 1535 cm^{-1}) show that a the linkage between the ammonium ions and phosphate ions [26]. In other words, the new $NH^{3+}–PO^{-}$ bond is formed due to one hydrogen atom of the amino group in chitosan is substituted by the

phosphate group. It further provides that the amino group is the only reactive functional group chitosan. Moreover, the characteristic peaks of the hydroxyl groups at 1377 cm^{-1} and 1322 cm^{-1} mentioned above do not change [24]. The cross-linked microparticles also show a new peak at 1217 cm^{-1} which may be attributed to the P=O stretching from TPP [27]. Therefore clearly indicating that the protonated amino groups of chitosan are linked with negatively charged tripolyphosphate groups of TPP, clearly demonstrating the formation of CS: TPP particles.

3.2. Crystallographic characterisation

Crystallographic structure of chitosan powder and chitosan microparticles were determined by X-Ray Diffraction (XRD). The XRD spectra of the chitosan microparticles were characteristic of amorphous structures. As can be seen in **Figure 2** there are two strong characteristic peaks in the diffractogram of chitosan powder at 2 θ = 10° (amine I "–N-CO-CH_3" of chitosan) and 2 θ = 20° (amine II "–NH_2" of chitosan), indicating the some degree of crystallinity of chitosan chains [28]. The peak at 10° is due to the integration of water molecules into the hydrated chitosan crystal structure and the latter peak at 20° is assigned to the crystal lattice of the chitosan orthorhombic unit cell (110) [29], furthermore there is no indication of impurities in the chitosan formulation [30]. It is known that the width of X-ray diffraction peak is related to the size of crystallite and an increase in the amorphous nature of the material [31]. Imperfect crystals usually lead to a broadened peak [32]. After ionic cross-linking with TPP, a shift of peak positions, significant reduction in the intensity of characteristic peaks of chitosan (at 2 θ = 20°), and broadening of peaks were observed, reflecting the destruction of the native chitosan packing structure [33]. **Figure 2** also highlights similarity between the CS: TPP ratios 2:1, 1:1, 1:2, 1:4 and 1:6. Therefore the broad peak of the chitosan microparticles is due to ionic cross-linking interaction between amino groups on chitosan and the TPP, which is known to destroy the crystalline structure of chitosan [33]. Integration of the two crystalline peaks (2 θ = 10 and 20°) as a proportion of the total integrated area gives an approximate estimate of the degree of crystallinity in each of the samples. Based on this calculation the degree of crystallinity of the native chitosan is ~ 30 % and the degrees of crystallinity of the TPP-chitosan microparticles are all ~10 %, this is almost entirely due to the decrease in the chitosan orthorhombic unit cell reflection (110) at ~ 20°. Other than for 6:1 and 4:1 the reflection (020) at ~ 10° remains unchanged during ionotropic gelation with TPP. Changes in chitosan crystallinity is important in terms of polymer degradation, tensile strength, moisture content, cell responses in *in vivo* applications and contact angles which are important during hydration. All of these are factors

are important to consider when developing novel chitosan-based formulations for forensic or pharmaceutical applications.

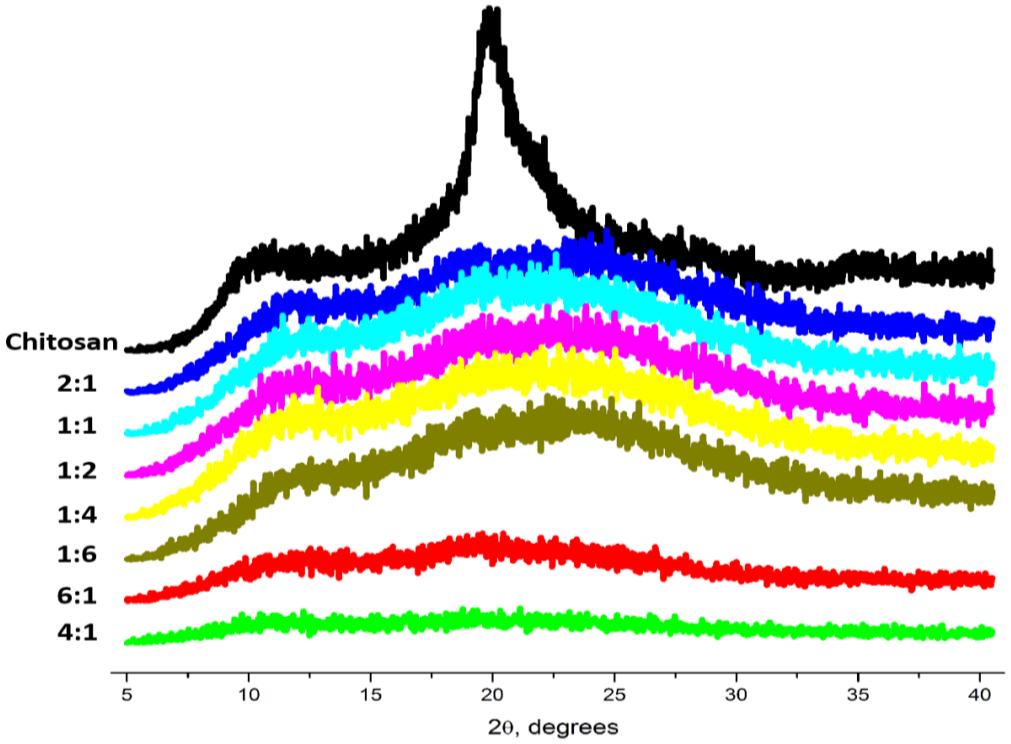

Figure 2. X-ray diffraction pattern of chitosan and of CS: TPP microparticles of different ratios in buffer AB-1. Only the diffraction pattern from 2θ = 5 - 40° is shown for clarity.

The cross linking of chitosan with a higher concentrations of TPP shows less intense and broader crystalline peaks (6:1 and 4:1) which may be due to a greater amorphisation as compared with those of less TPP 2:1, 1:1, 1:2, 1:4 and 1:6 [28]. The distinct differences in the diffractogram of chitosan and cross-linked chitosan might be attributed to chemical modification in the arrangement of molecules in the crystal lattice [26] and this is also in agreement with FT-IR as to the absence of "native" chitosan.

3.3. Relative viscosity and zeta potential for varying chitosan solutions

Chitosan when in solution is a polycation which is influenced by the presence of electrolytes [34]. Thus, the effect of ionic strength and pH value on nine different solutions of chitosan was studied. It can be seen from **Figure 3A** that the relative viscosity of nine chitosan solutions, with fixed pH including AB-1, AB-2 and AB-3; AB-4, AB-5 and AB-6; AB-7, AB-8 and AB-9 decreased with increasing ionic strength solution.

Chain flexibility of chitosan molecules in solution can be manipulated by using chitosan with differing solution pH and/or ionic strength. Furthermore, it is known that in acidic media the amino groups of chitosan, $–NH_2$, are protonated to $–NH_3^+$ groups. This causes electrostatic repulsion between chitosan molecules; meanwhile, there also exists inter-chain hydrogen bonding interactions between chitosan molecules. The hydrogen bonding occurs between the amino and hydroxyl groups [35].

In low ionic strength solutions (0.1 M), the intramolecular electrostatic repulsion effect, also called the third electroviscous effect, dominates in which the chitosan molecule exists in an extended conformation [35, 36]. Therefore, more inter-molecular hydrogen bonding occurs in low ionic strength solution [37]. This causes a high resistance to the flow or mobility of the polymer molecules and consequently a high relative viscosity is observed. However, in high ionic strength solutions (0.5 M), the concentration of acetate ions (CH_3COO^-) is raised which neutralises more $-NH_3^+$ groups. This leads to less dissolution of chitosan and weaker intermolecular electrostatic repulsion, causing the chitosan polymer chains to become more contracted and lowers the resistance to the flow or mobility of the polymers, resulting in a lower relative viscosity [38]. In addition, the relative viscosity of chitosan also decreased with increasing pH in solutions with fixed ionic strength. The number of positive charges on CS at I.S 0.1 M will be greater at pH 3.3 of the solvent, leading to a higher degree of expansion of chitosan and a rigid conformation due to electrostatic repulsions [39]. Information on chain expansion of chitosan used in the formulation of microparticles enables the possibility to better control microparticle properties by selecting suitable preparation conditions or starting polymer [40]. Because of this, the chitosan molecules disrupt the streamlining of the flow and increases viscosity, which will have an influence on the size (and shape) of any chitosan microparticles formed under these conditions [41].

Zeta potential measurement is important to gain knowledge on the surface charge. This charge can affect the interaction between chitosan polymer chains in phenomena such as swelling , in the interaction with TPP during gelation [42] or during the interaction with oily subcutaneous residues [7]. The ionic strength and pH value of the chitosan solution affect this interaction.

The effect of pH value and ionic strength of the chitosan solution on zeta potential may be seen:

(i) At variable pH value and fixed ionic strength

It can be seen from **Figure 3B** that the zeta potential decreases as the pH value increases from 3.3 to 5.3. At pH 3.3, the primary amine groups -NH_2 of chitosan are more strongly protonated as -NH_3^+ in acetate buffer solution and therefore increased zeta potential. On the other hand, at an increased pH value of 5.3 the –NH_3^+ on the chitosan molecules were more neutralised resulting in a decreased zeta potential.

(ii) At the fixed pH value and variable ionic strength (0.1, 0.3 and 0.5 M)

It can be seen from **Figure 3B** that the zeta potential decreased with an increase in the ionic strength from 0.1 M to 0.5 M. At ionic strength 0.1 M, the primary amine groups -NH_2 of chitosan are protonated as -NH_3^+ in acetate buffer solution and therefore an increased zeta potential is seen. Conversely, with an increased ionic strength at 0.5 M, the –NH_3^+ on the chitosan molecules were charge screened by acetate ions (CH_3COO^-) leading to a decreased zeta potential. This is important in terms of the conformation of chitosan chains and how that might influence their interactions with TPP polyanions during ionotropic gelation where the change in zeta potential of chitosan (and indeed all polyelectrolyte biopolymers) can be used to estimate chain stiffness [36].

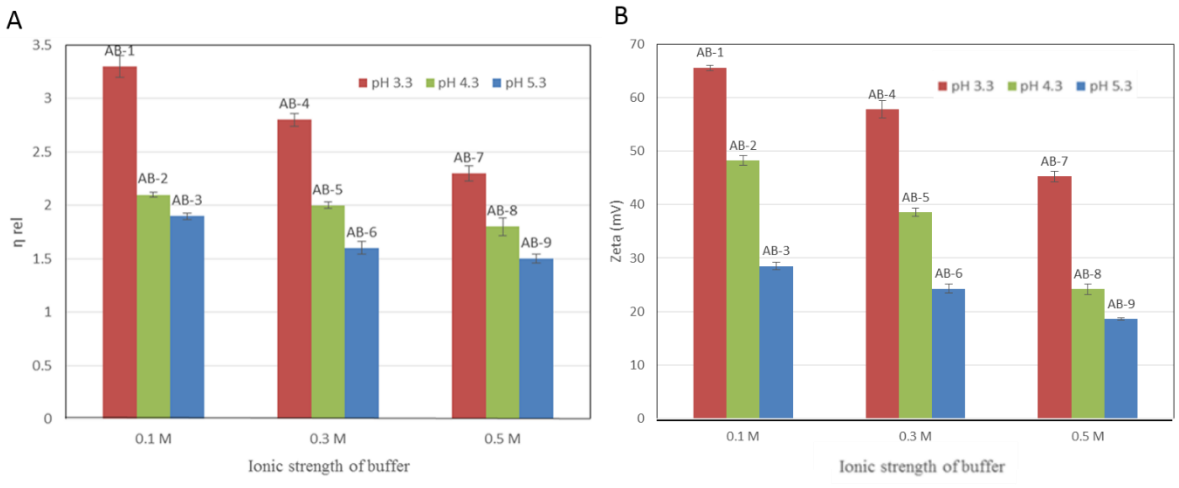

Figure 3. Relative viscosities (**A**) and zeta potentials (**B**) of nine different chitosan solutions (using AB-1 to AB-9) at varying ionic strength and pH values at 25.0 ± 0.1 ^oC (mean ± STDEV, n = 3).

3.4. Analysis of different ratios of CS: TPP microparticles with different acetate buffers

In this study CS: TPP microparticles formed by ionotropic gelation, were prepared at various ratios, (loaded with red dye for visualisation purposes), by the mixing CS solution with TPP solution under stirring. The particles formed at each ratio were shown to have different chemical and physical properties (**Figure 4 A-G**). As can be seen in **Figure 4**, microparticles prepared with AB-12 at the higher CS: TPP ratios and therefore at higher viscosity and surface charge had more porous surfaces than those of microparticles prepared with the lower CS: TPP ratios which had irregular angular surfaces, this is expected to have an influence strength of interaction and therefore integrity of the particle "walls" and therefore their size and shape [43]. The availability of TPP is of course limited at high chitosan ratios and in excess in those with lower chitosan ratios and this influences the cross-linking density which again has an effect on size, shape and morphology of the particles [43]. Furthermore, although it may appear as though some of the particles are fragments of precipitated chitosan this is not the case as this inconsistent with both the FT-IR and XRD data above. In terms of potential applications of non-spherical particles it has been previously reported that flake-like metal particles (aluminium, copper, *etc*.) are more effective than spherical particles in latent fingerprint development [8] due to increased surface: volume ratios [7], therefore samples with a 2:1 CS: TPP ratio were used for further forensic studies in latent fingerprint visualisation with encouraging results (Hejjaji, Smith and Morris, submitted), this will depend on total particle surface area, which ranges from ~7000 μm^2 (**Figure 4D**) to >30000 μm^2 (**Figure 4A**) and on the number of particles per unit area. In the case of the irregular particles previous research has shown that the shape of CS: TPP microparticles depends on the pH at which chitosan and TPP are mixed and the molecular weight (viscosity) of the chitosan [44], furthermore in terms of pharmaceutical applications irregular particles with angular features have been shown to decrease drug dissolution [45], have a higher drug loading efficiency [46], influence phagocytosis [47] and to have a greater probability of adhering to cancer cell surfaces [48] which suggests that CS: TPP microparticles formed in this way may be have potential in drug delivery formulations. Although due to the inherent difficulties in measuring particles with different morphologies the impact of shape has not been studied to a great extent.

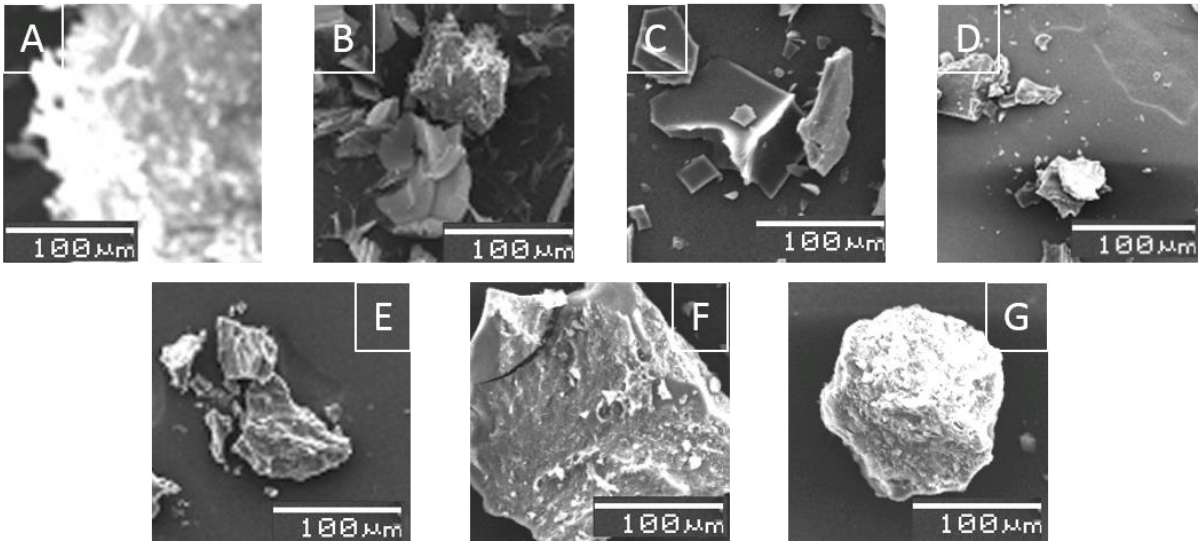

Figure 4. Example SEM images at 20 kV of chitosan microparticles CS: TPP using AB-12 (A) 6:1, (B) 4:1, (C) 2:1, (D) 1:1, (E) 1:2, (F) 1:4 and (G) 1:6. Where the scale bar is 100 μm and the estimated total surface areas of the particles are approximately ~30000, 14000, 8000, 7000, 8000, 32000 and 15000 μm^2, respectively.

The relative viscosity of the CS: TPP microparticle suspension is shown in **Figure 5A**, which indicates that neither pH nor ionic strength have a large influence the relative viscosity at ratios CS: TPP 1:6, 1:4, 1:2, 1:1 and 2:1. It can be attributed to its lesser resistance towards flow due the relatively low charge on chitosan microparticles. At higher ratios (4:1; 6:1), the relative viscosity is higher with an increase in the CS: TPP ratio in the mixture. Moreover, at the fixed pH value and different ionic strength (0.1, 0.3 and 0.5 M), the relative viscosity increased with a decrease in ionic strength. This behaviour may arise because of the decrease in the repulsion force between charges for the solvent and polymers and not unsurprisingly is dominated by the amount of chitosan in the microparticles.

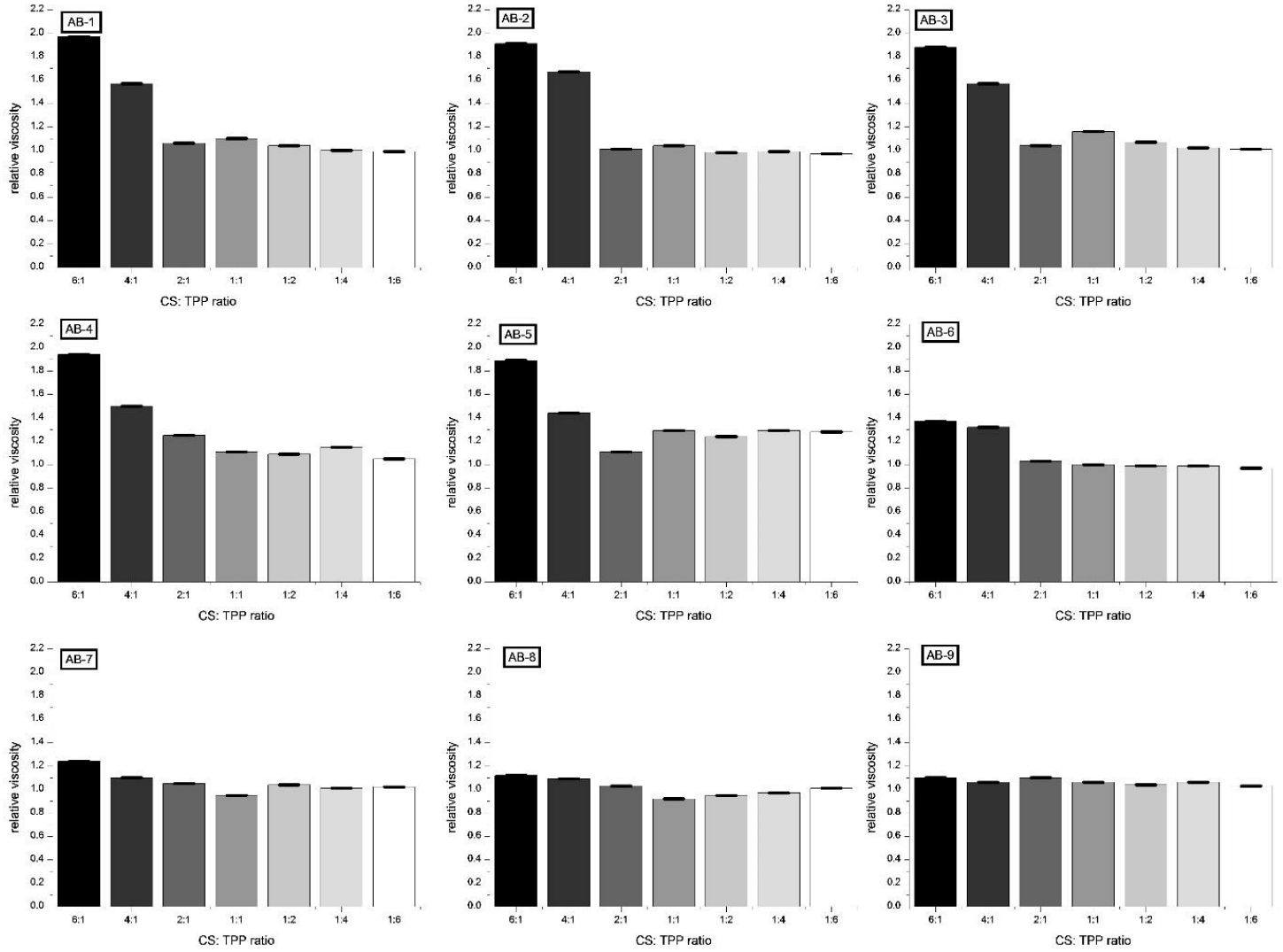

Figure 5A. Relative viscosities of CS: TPP microparticles solutions (using AB-1 to AB-9) at varying ionic strength and pH values at 25.0 ± 0.1 ^{o}C (mean ± STDEV, n = 3).

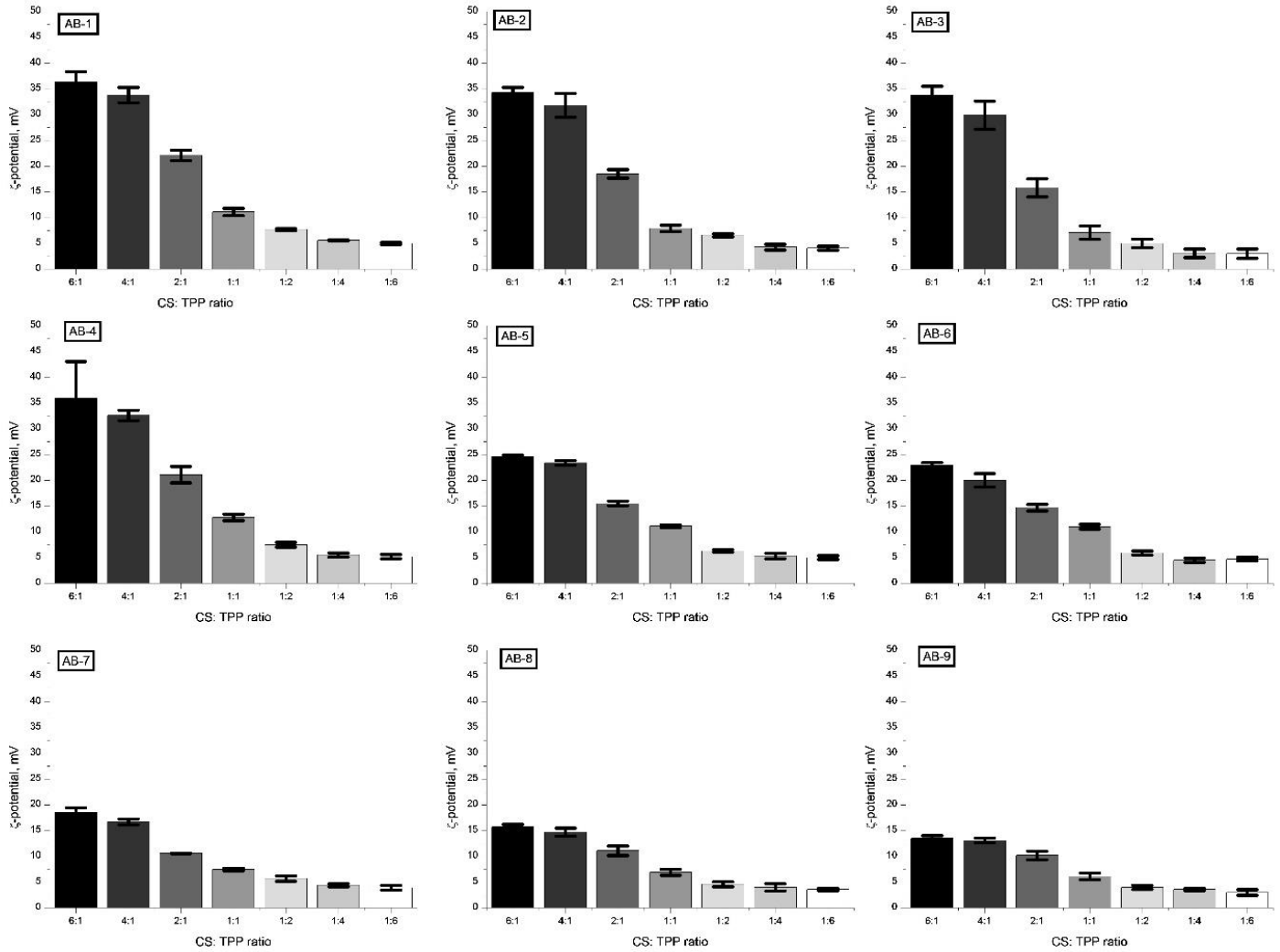

379

380 **Figure 5B.** Zeta potentials of CS: TPP microparticles solutions (using AB-1 to AB-9) at varying ionic strength and pH values at 25.0 ± 0.1 ºC

381 (mean ± STDEV, n = 3).

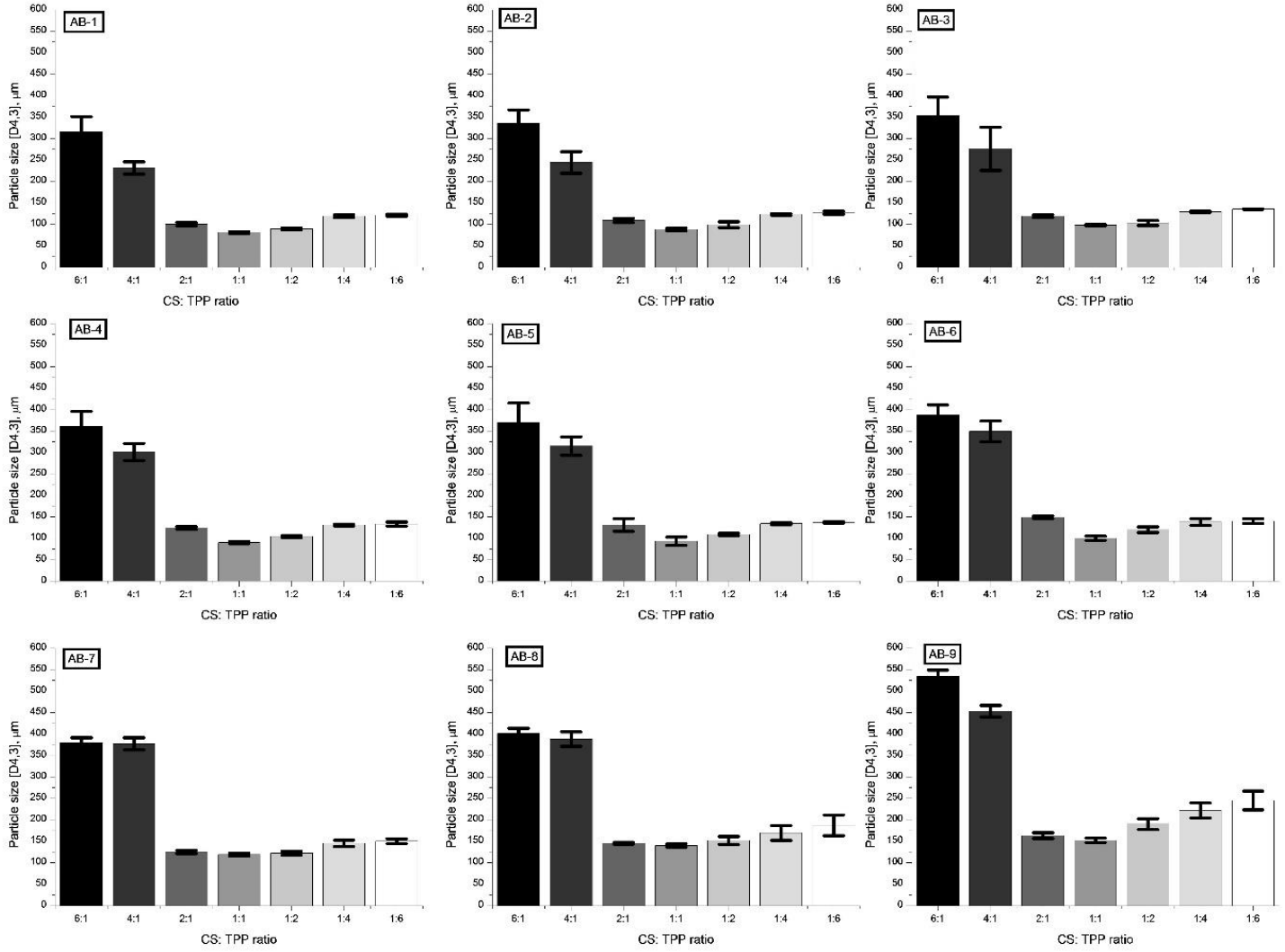

382

383 **Figure 5C.** Particle size ($D_{[4,3]}$) of CS: TPP microparticles solutions (using AB-1 to AB-9) at varying ionic strength and pH values at 25.0 ± 0.1

384 ^{o}C (mean ± STDEV, n = 3).

The effect of ionic strength and pH value on the zeta potential of nine chitosan microparticle formulations was investigated as shown in **Figure 5B**. When chitosan and TPP were mixed with each other in an acetate buffer, they spontaneously formed microparticles (diameters were in the range 28-445 μm) with an overall positive surface charge which are at least partially within the size range of particles which have been demonstrated to be effective in latent fingerprint visualisation ~1-50 μm [8] and may have potential in pulmonary [40] or colonic drug delivery systems[49] . The more positively or negatively charged the particles, the more they repel each other and therefore at values of ± 30 mV are required for optimal stability [50]. As the CS: TPP ratio decreased from 6:1 to 1:6 the zeta potential values decreased from for example 36.4 mV to 5 mV in buffer AB-1 or from 13.5 mV to 3 mV in buffer AB-9 (**Figure 5B**). It was also observed that with a decrease in the concentration of chitosan the appearance of the system changed from clear viscous liquid to milky dispersion prior to precipitation.

It was demonstrated that, there was no significant difference in the zeta potential values of CS: TPP from 1:2 to 1:6, indicating neutralization of the protonated amino groups on the surface of chitosan microparticles and subsequent loss of repulsive force which led to precipitation of the particles. On the other hand, as the CS: TPP ratio increased from 1:2 to 6:1 the zeta potential increased almost linearly. The large positive surface charge due to the high degree of deacetylation and protonation causes the chitosan molecules to have a large number of potential cross-linking sites. The presence of higher positive charge on the particles indicated that free (non-cross-linked) amino groups remained on the particle surface [35, 51] which is consistent with an increased viscosity in solution.

When the CS: TPP ratio was high at 6:1and 4:1 (the available quantity of TPP was small) the reaction solution was clear, indicating that the amount of phosphate groups was inadequate to lead to the full cross-linking with the chitosan amino groups [52]. As the CS: TPP ratio decreased from 6:1 to 1:1, the particle size decreased due to increased intramolecular and intermolecular cross-linking density between chitosan amino groups and the TPP groups (**Figure 5C**), this is also due to the decrease in viscosity (**Figure 5A**) which leads weaker networks and therefore assuming there is no change in shear forces (stirring rate was constant at 600 rpm in all cases) smaller particles [41]. It can be inferred that chitosan molecules were almost fully cross-linked at CS: TPP (1:1), which coincided with the smallest particle size range measured. As the CS: TPP ratio decreases further from 1:1 to 1:6 the particle size increased, as

more TPP molecules are involved in the formation of the microparticles. This increased concentration of TPP promotes aggregation due to inter-particle cross-linking (bridging effects) which leads to a lower surface charge density of the particles resulting in precipitation [52]. As we can see in **Figure 4** the CS: TPP microparticles are in some cases non-spherical, with aspect ratios ranging from 1:1 to 13:1 and as particle size analysis treats particles as equivalent spheres there is potential for minor discrepancies in the absolute particle sizes, these are expected to be minimal although this will depend on the type of material being measured [53].

Using multiple regression analysis, the responses (relative viscosity, zeta potential and particle size) were correlated with the three variables studied using second-order polynomials. The coefficients of the model equation and their statistical significance were evaluated using Minitab® 17.1.0 software (Minitab Inc., Philadelphia, U.S.A.). The regression model for the responses to relative viscosity (Y_1), zeta potential (Y_2) and particle size (Y_3) in terms of coded factors is given by Equations 2 - 4 respectively.

$$Y_1 = -0.251 + 0.575\,X_1 - 0.136\,X_2 + 0.3315\,X_3 - 0.0631\,X_1^2 + 0.008\,X_1X_2 - 0.0676\,X_1X_3 + 0.232\,X_2^2 - 0.178\,X_2X_3 + 0.01397\,X_3^2 + 0.0213\,X_1X_2X_3 \quad (2)$$

$$Y_2 = -25.54 + 14.89\,X_1 - 35.8\,X_2 + 15.00\,X_3 - 1.812\,X_1^2 + 6.88\,X_1X_2 - 1.606\,X_1X_3 + 16.5\,X_2^2 + 2.32\,X_2X_3 - 0.5282\,X_3^2 - 1.446\,X_1X_2X_3 \quad (3)$$

$$Y_3 = 299 - 98.3\,X_1 - 271\,X_2 - 9.9\,X_3 + 12.4\,X_1^2 + 54.5\,X_1X_2 + 4.23\,X_1X_3 + 167\,X_2^2 - 12.2\,X_2X_3 + 5.50\,X_3^2 + 7.1\,X_1X_2X_3 \quad (4)$$

The equations were applied the response, to describe the principal effects and interactions amongst the identified variables pH (X_1), ionic strength (X_2) and ratio (X_3).

The coefficients with one factor represent the effect of the particular factor, while the coefficients with two factors, three factors and those with second order terms represent the interaction between the two factors, three factors and quadratic effect, respectively. The positive sign in front of the terms indicates synergistic effect, while negative sign indicates antagonistic effect on the responses.

3.5. Model validation of relative viscosity, zeta potential and particle size

Four different chitosan microparticles formulations were prepared in different acetate buffers including AB-10, AB-11, AB-12 and AB-13. The relative viscosities and zeta potential of the four chitosan microparticles were measured (**Table 2**). The regression equations were obtained for equations 2 - 4 which suggests the empirical relationship between the value of response and the independent variable. Therefore, the predicted values were calculated using mathematical model from equations 2 - 4.

For validation of relative viscosity, zeta potential and particle size results, the experimental values of the responses were compared with that of the predicted values **Table 2**. Moreover, **Table 2** indicates that ionic strength, pH and Chitosan: TPP ratio are suitable in predicting viscosity, zeta potential and particle size due to a high values of r^2, (r^2 = 0.91, r^2 = 0.96 and 0.86 respectively) and can therefore be used in future studies to design tuneable microparticles for specific applications.

Table 2. Observed (Exp.) responses and predicted (Pred.) values for relative viscosity (Y_1), zeta potential (Y_2) and particle size (Y_3)

Dependant Variables			Y_1 Relative viscosity		Y_2 Zeta potential (mV)		Y_3: Particle size [$D_{4,3}$] (μm)	
X_1 pH	X_2 I.S.	X_3 (CS:TPP) Ratio	Exp.	Pred.	Exp.	Pred.	Exp.	Pred.
3.8	**0.2**	**6:1**	1.66 ± 0.01	1.85	35.2 ± 1.3	34.2	354 ± 40	351
3.8	**0.2**	**4:1**	1.34 ± 0.01	1.46	29.7 ± 1.1	28.2	226 ± 21	223
3.8	**0.2**	**2:1**	1.07 ± 0.01	1.18	19.0 ± 1.6	18.0	135 ± 6	139
3.8	**0.2**	**1:1**	1.11 ± 0.01	1.08	11.8 ± 0.9	11.3	111 ± 3	113
3.8	**0.2**	**1:2**	1.05 ± 0.01	1.04	8.5 ± 1.3	7.6	119 ± 2	104
3.8	**0.2**	**1:4**	1.04 ± 0.01	1.03	6.1 ± 0.9	5.6	124 ± 3	101
3.8	**0.2**	**1:6**	1.04 ± 0.01	1.02	5.8 ± 0.4	5.0	128 ± 6	100
3.8	**0.4**	**6:1**	1.66 ± 0.01	1.74	32.6 ± 2.9	30.4	379 ± 49	376
3.8	**0.4**	**4:1**	1.45 ± 0.01	1.38	27.0 ± 2.7	25.7	248 ± 41	242
3.8	**0.4**	**2:1**	1.04 ± 0.01	1.15	17.0 ± 0.6	16.8	146 ± 5	152
3.8	**0.4**	**1:1**	1.00 ± 0.01	1.07	10.0 ± 0.7	10.8	121 ± 2	123
3.8	**0.4**	**1:2**	1.02 ± 0.01	1.04	8.0 ± 1.2	7.3	129 ± 5	113
3.8	**0.4**	**1:4**	1.02 ± 0.01	1.03	6.0 ± 1.4	5.5	132 ± 4	109
3.8	**0.4**	**1:6**	1.02 ± 0.01	1.02	4.3 ± 0.7	4.9	135 ± 5	108
4.8	**0.2**	**6:1**	1.45 ± 0.01	1.50	21.3 ± 0.4	23.5	407 ± 50	404
4.8	**0.2**	**4:1**	1.24 ± 0.01	1.24	19.9 ± 0.8	21.3	267 ± 31	265
4.8	**0.2**	**2:1**	1.09 ± 0.01	1.08	14.3 ± 0.6	14.9	171 ± 4	169
4.8	**0.2**	**1:1**	1.03 ± 0.01	1.05	9.7 ± 0.5	10.1	135 ± 2	138
4.8	**0.2**	**1:2**	0.98 ± 0.01	1.04	8.0 ± 0.1	7.3	138 ± 2	126
4.8	**0.2**	**1:4**	1.07 ± 0.01	1.04	6.9 ± 0.4	5.8	139 ± 2	122
4.8	**0.2**	**1:6**	0.97 ± 0.01	1.04	4.8 ± 0.1	5.4	142 ± 6	120
4.8	**0.4**	**6:1**	1.38 ± 0.01	1.42	18.6 ± 0.6	19.4	451 ± 31	445
4.8	**0.4**	**4:1**	1.21 ± 0.01	1.18	17.3 ± 0.1	19.0	306 ± 29	300
4.8	**0.4**	**2:1**	1.06 ± 0.01	1.06	10.3 ± 0.3	14.5	194 ± 11	196
4.8	**0.4**	**1:1**	1.02 ± 0.01	1.04	9.0 ± 0.5	10.6	158 ± 8	161
4.8	**0.4**	**1:2**	0.98 ± 0.01	1.05	6.8 ± 0.3	8.3	164 ± 10	147
4.8	**0.4**	**1:4**	1.02 ± 0.01	1.05	5.7 ± 0.2	7.0	167 ± 23	141
4.8	**0.4**	**1:6**	0.98 ± 0.01	1.05	4.2 ± 0.5	6.6	171 ± 15	139

4. Conclusions

In this study, chitosan microparticles of different morphologies were successfully formed by the ionotropic gelation method at different CS: TPP ratios and pH/Ionic strength conditions. The particles were characterized by relative viscosity, zeta potential, particle size, FTIR spectroscopy and XRD. Using experimental design, the relative viscosity, particle size and zeta potential of CS: TPP microparticles under different conditions could be predicted using the

mathematical models. The mathematical models obtained showed good relationships between independent variables (pH, ionic strength and CS: TPP ratio) and dependent variables (relative viscosity, zeta potential and particle size) for prediction. This gives us the ability to design tuneable CS-TPP microparticles for specific pharmaceutical or forensic applications more specifically latent fingerprint visualisation.

5. Acknowledgements

The authors would like to thank the University of Huddersfield and the Libyan Government for funding this study.

6. References

[1] A.K. Sailaja, P. Amareshwar, P. Chakravarty, Research Journal of Pharmaceutical, Biological and Chemical Sciences, 1 (2010) 474-484.

[2] G.A. Morris, J. Castile, A. Smith, G.G. Adams, S.E. Harding, Carbohydrate Polymers, 76 (2009) 616-621.

[3] T.K. Giri, A. Thakur, A. Alexander, H. Badwaik, D.K. Tripathi, Acta Pharmaceutica Sinica B, 2 (2012) 439-449.

[4] A. Shweta, P. Sonia, International Research Journal of Pharmacy, 4 (2013) 45.

[5] G.A. Morris, S.M. Kök, S.E. Harding, G.G. Adams, Biotechnology and Genetic Engineering Reviews, 27 (2010) 257-284.

[6] I. Il Dueik, G.A. Morris, International Journal of Carbohydrate Chemistry, 2013 (2013).

[7] B. Yamashita, M. French, Latent print development, in: E.H. Holder, L.O. Robinson, J.H. Laub (Eds.) The fingerprint sourcebook, U.S. Department of Justice, Washington, DC, USA, 2011, pp. 1-67.

[8] J.D. James, C.A. Pounds, B. Wilshire, Journal of Forensic Science., 36 (1991) 1368-1375.

[9] J.J. Wang, Z.W. Zeng, R.Z. Xiao, T. Xie, G.L. Zhou, X.R. Zhan, S.L. Wang, International Journal of Nanomedicine, 6 (2011) 765-774.

[10] S. Jarudilokkul, A. Tongthammachat, V. Boonamnuayvittaya, Korean Journal of Chemical Engineering, 28 (2011) 1247-1251.

[11] A.M. Dyer, M. Hinchcliffe, P. Watts, J. Castile, I. Jabbal-Gill, R. Nankervis, A. Smith, L. Illum, Pharmaceutical Research, 19 (2002) 998-1008.

[12] P. He, S.S. Davis, L. Illum, Journal Microencapsulation, 16 (1999) 343-355.

[13] K.A. Janes, P. Calvo, M.J. Alonso, Adv. Drug Deliv. Rev., 47 (2001) 83-97.

[14] G.A. Morris, J. Castile, A. Smith, G.G. Adams, S.E. Harding, Carbohydrate Polymers, 84 (2011) 1430-1434.

[15] A. Rampino, M. Borgogna, P. Blasi, B. Bellich, A. Cesaro, International Journal of pharmaceutics, 455 (2013) 219-228.

[16] X.Z. Shu, K.J. Zhu, International Journal of Pharmaceutics, 201 (2000) 51-58.

[17] A. Dyer, M. Hinchcliffe, P. Watts, J. Castile, I. Jabbal-Gill, R. Nankervis, A. Smith, L. Illum, Pharmaceutical Research, 19 (2002) 998-1008.

[18] G.A. Morris, J. Castile, A. Smith, G.G. Adams, S.E. Harding, Carbohydrate Polymers, 84 (2011) 1430-1434.

[19] S.E. Harding, Progress in Biophysics and Molecular Biology, 68 (1997) 207-262.

[20] D.E. Azofeifa, H.J. Arguedas, W.E. Vargas, Optical Materials, 35 (2012) 175-183.

[21] A.R. Dudhani, S.L. Kosaraju, Carbohydrate Polymers, 81 (2010) 243-251.

519 [22] A.F. Martins, D.M. de Oliveira, A.G. Pereira, A.F. Rubira, E.C. Muniz, International Journal of
520 Biological Macromolecules, 51 (2012) 1127-1133.
521 [23] S.W. Ali, S. Rajendran, M. Joshi, Carbohydrate Polymers, 83 (2011) 438-446.
522 [24] K. Wang, Q. Liu, Carbohydrate Research, 386 (2014) 48-56.
523 [25] Y. Wu, W. Yang, C. Wang, J. Hu, S. Fu, International Journal of Pharmaceutics, 295 (2005) 235-245.
524 [26] D.R. Bhumkar, V.B. Pokharkar, AAPS PharmSciTech, 7 (2006) E138-E143.
525 [27] L. Qi, Z. Xu, Colloids and Surfaces A: Physicochemical and Engineering Aspects, 251 (2004) 183-
526 190.
527 [28] M. Moharram, F. Reicha, N. Kinawy, W. El Hotaby, Journal of Applied Sciences Research, 8 (2012).
528 [29] M. Matet, M.C. Heuzey, E. Pollet, A. Ajji, L. Avérous, Carbohydrate Polymers, 95 (2013) 241-251.
529 [30] M. Lad, T. Todd, G.A. Morris, W. Macnaughtan, G. Sworn, T.J. Foster, Food Chemistry, 139 (2013)
530 1146-1151.
531 [31] J.W. Rhim, S.I. Hong, H.M. Park, P.K.W. Ng, Journal of Agricultural and Food Chemistry, 54 (2006)
532 5814-5822.
533 [32] J. Jingou, H. Shilei, L. Weiqi, W. Danjun, W. Tengfei, X. Yi, Colloids and Surfaces B: Biointerfaces,
534 83 (2011) 103-107.
535 [33] S.F. Hosseini, M. Zandi, M. Rezaei, F. Farahmandghavi, Carbohydrate Polymers, 95 (2013) 50-56.
536 [34] O. Smidsrod, A. Haug, Biopolymers, 10 (1971) 1213-1227.
537 [35] W. Fan, W. Yan, Z. Xu, H. Ni, Colloids and Surfaces B: Biointerfaces, 90 (2012) 21-27.
538 [36] A. Abodinar, A.M. Smith, G.A. Morris, Carbohydrate Polymers, (2014).
539 [37] G. Qun, W. Ajun, Carbohydrate Polymers, 64 (2006) 29-36.
540 [38] B. Hu, C. Pan, Y. Sun, Z. Hou, H. Ye, X. Zeng, Journal of Agricultural and Food Chemistry, 56 (2008)
541 7451-7458.
542 [39] M.R. Kasaai, J. Arul, G. Charlet, Journal of Polymer Science Part B: Polymer Physics, 38 (2000)
543 2591-2598.
544 [40] B. Bellich, I. D'Agostino, S. Semeraro, A. Gamini, A. Cesàro, Marine Drugs, 14 (2016).
545 [41] J. Kawadkar, M.K. Chauhan, European Journal of Pharmaceutics and Biopharmaceutics., 81 (2012)
546 563-572.
547 [42] Q. Gan, T. Wang, C. Cochrane, P. McCarron, Colloids Surfaces B Biointerfaces, 44 (2005) 65-73.
548 [43] R. Ponnuraj, K. Janakiraman, S. Gopalakrishnan, K. Senthilnathan, V. Meganathan, P. Saravanan,
549 Indo American Journal of Pharmaceutical Research, 5 (2015) 387-399.
550 [44] J.A. Ko, H.J. Park, S.J. Hwang, J.B. Park, J.S. Lee, International Journal of Pharmaceutics, 249 (2002)
551 165-174.
552 [45] M. Mosharraf, C. Nyström, International Journal of Pharmaceutics, 122 (1995) 35-47.

553 [46] V. Uskoković, K. Lee, P.P. Lee, K.E. Fischer, T.A. Desai, ACS Nano, 6 (2012) 7832-7841.
554 [47] J.A. Champion, Y.K. Katare, S. Mitragotri, Journal of Controlled Release, 121 (2007) 3-9.
555 [48] Y. He, K. Park, Molecular Pharmaceutics, (2016).
556 [49] E.M. Collnot, H. Ali, C.M. Lehr, Journal of Controlled Release, 161 (2012) 235-246.
557 [50] D.-W. Tang, S.-H. Yu, Y.-C. Ho, B.-Q. Huang, G.-J. Tsai, H.-Y. Hsieh, H.-W. Sung, F.-L. Mi, Food
558 Hydrocolloids, 30 (2013) 33-41.
559 [51] H. Zhang, M. Oh, C. Allen, E. Kumacheva, Biomacromolecules, 5 (2004) 2461-2468.
560 [52] J. Li, Q. Huang, Carbohydrate Polymers, 87 (2012) 1670-1677.
561 [53] C. Polakowski, A. Sochan, A. Bieganowski, M. Ryzak, R. Földényi, J. Tóth, International
562 Agrophysics., 28 (2014) 195-200.
563